RSC Advances

ROYAL SOCIETY OF CHEMISTRY

www.rsc.org/advances

Three 3D frameworks built from strip-shaped Δ-chains with mixed double bridges were prepared and magnetically characterized. They show different bulk magnetic behaviors: the Cu(II) compound shows spin canting, giving rise to magnetic ordering and metamagnetism, while the Co(II) and Ni(II) compounds show canted antiferromagnetism, respectively.

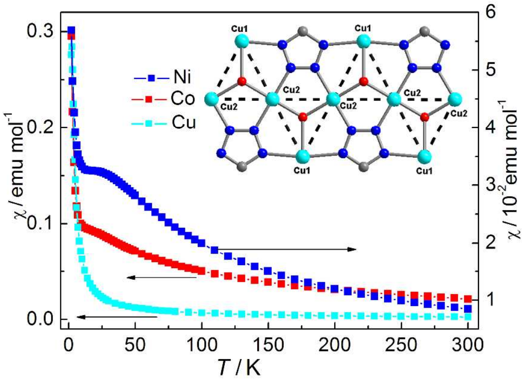

RSC Advances

Cite this: DOI: 10.1039/c0xx00000x

www.rsc.org/xxxxxx

ARTICLE TYPE

# Spin-canting magnetization in 3D metal organic frameworks based on strip-shaped Δ-chains

***Xiu-Mei Zhang,* Peng Li, Wei Gao, and Jie-Ping Liu***

***Received (in XXX, XXX) Xth XXXXXXXXX 200X, Accepted Xth XXXXXXXXX 200X***

**DOI:**

Three isostrustural coordination polymers, $M_2(TZI)(OH)(H_2O)_2{\cdot}xH_2O$ (x = 3, M= Cu(II) **1**, x = 4 M = Co(II) **2** and Ni(II) **3**) ($H_3TZI$ = 5-(1H-tetrazol-5-yl)isophthalic acid), have been synthesized under hydrothermal conditions. The compounds consist of 3D frameworks, in which the magnetic Δ-chain motifs based on corner-sharing $M_3(\mu_3\text{-}OH)$ isosceles triangle are linked by the TZI ligands, and they represent the rare (3,4,5,6)-connected 4-nodal net topology with the point symbol $(4^3)(4^46^2)(4^66^4)(4^76^8)$. Magnetic analyses indicate that compound **1** shows the coexistence of spin canting, metamagnetism and antiferromagnetic ordering, whereas compounds **2** and **3** exhibit canted antiferromagnetic coupling without magnetic ordering down to 2 K. Such magnetic behaviors above 2 K are still a rarity in Cu(II), Co(II) and Ni(II) compounds with similar chains.

## Introduction

Molecular magnetism has attracted much attention in recent years due to their great value in understanding the fundamental magnetic phenomena, revealing the magnetostructural relationships, and constructing new molecular magnetic materials with potential technological applications.[1-3] In particular, the studies have been much promoted by the discoveries of magnetic materials with spontaneous magnetization, such as spin canting, metamagnetism and long-range magnetic ordering. It is well-known that spin canting system can arise from two mechanisms: single-ion anisotropy and the antisymmetric Dzyaloshinsky-Moriya (DM) interaction.[4] They both require that there is no inversion center between the interacting spins. Therefore, the antiferromagnetic (AFM) and ferromagnetic (FM) coupling between the noncollinear alignment of the spins usually result in spin-canting magnetic behaviors.[5] Metamagnetism requires that the chain/layer must have net moments and may be FM or ferrimagnetic (FIM) or AFM with spin canting, and the interchain/interlayer interactions can induce AF ordering and are to be overcome by a critical field.[6] Magnetic materials, especially, those displaying canted metamagnetic ordering, are viewed as one of the good candidates of molecular magnets. However, the design and synthesis of such magnetic materials are still a challenging task. The selection of the short bridging ligands between paramagnetic centers is very important; because they may transmit magnetic coupling and build the secondary building units (SBUs) to construct novel structural topology. The tetrazole and carboxylate as short bridging ligands have attracted much attention due to their coordinative and magnetic versatility. They can bind metal ions in various bridging modes and efficiently induce either FM or AFM coupling.[7,8] To date, several Co(II) molecular magnets with tetrazole and $\mu_3$-OH bridged magnetic Δ-chains have been synthesized, including metamagnetism, spin-canting and long-range ordered systems.[9] But the only one known Cu(II) species[10] with the similar chains has been reported, which displays spin-frustrated antiferromagnetic ordering. We are interested in 5-(1H-tetrazol-5-yl)isophthalic acid ($H_3TZI$), which has several remarkable features as follows: (i) two carboxylate groups may bind to metal centers with various coordination modes, allowing for varied magnetic interactions; (ii) The tetrazolate groups are expected to construct frustrated triangular motifs; (iii) Both the carboxylate and tetrazolate groups of $H_3TZI$ have the ability to connect metal ions into high dimensional networks. Despite a few compounds with this liand have been reported[11], it remains largely unexplored. Here we report three isostrustural coordination polymers with this ligand, $M_2(TZI)(OH)(H_2O)_2{\cdot}xH_2O$ (x = 3, M= Cu(II) **1**, x = 4 M = Co(II) **2** and Ni(II) **3**) ($H_3TZI$ = 5-(1H-tetrazol-5-yl)isophthalic acid), in which the strip-shaped Δ-chains motifs built from corner-sharing $M_3(\mu_3\text{-}OH)$ triangle units with mixed double ($\mu_4$-tetrazolate)($\mu_3$-OH) bridges. Compounds represent the rare (3,4,5,6)-connected 4-nodal net topology with the point symbol $(4^3)(4^46^2)(4^66^4)(4^76^8)$. Magnetic investigations indicated that they all display intrachain spin canting AFM interactions through the mixed double bridges but the bulk behaviors are different. Compound **1** exhibit spin-canted ordering and metamagnetism, whereas compounds **2** and **3** exhibit canted antiferromagnetic coupling without magnetic ordering down to 2 K, respectively. Noticeably, the complex magnetic phenomena of **1**, **2** and **3** are different from previous compounds with similar chains.

## Experimental

### Materials and physical measurements

All the solvents and reagents including 5-(1H-tetrazol-5-yl)isophthalic acid ($H_3TZI$) were purchased commercially and were used as received. Infrared spectra were recorded on a NEXUS 670 FT-IR spectrometer using the KBr pellets. Elemental analysis was carried out in the range 500- 4000 $cm^{-1}$ on an Elementar Vario El III elemental analyzer. The phase purity of the samples was confirmed by powder X-ray diffraction collected on a Bruker D8-ADVANCE diffractometer equipped with Cu Kα at a scan speed of 1° $min^{-1}$. Temperature-dependent and field-dependent magnetic measurements were carried out on a Quantum Design SQUID MPMS-5 magnetometer. Diamagnetic corrections were made with Pascal's constants.

**$[Cu_2(OH)(TZI)(H_2O)_2]_n·3nH_2O$** (**1**). A mixture of $Cu(NO_3)_2·3H_2O$ (0.024 g, 0.1 mmol), and $H_3TZI$ (0.023 g, 0.1 mmol) in $H_2O/CH_3CN$ (6/6 mL) was stirred for 10 min at room temperature, then sealed in a Teflon-lined stainless steel vessel (25 mL), heated at 150°C for 2 days under autogenous pressure, and then cooled to room temperature, blue crystals of **1** were obtained. Yield, 53% based on Cu. Elem anal. Calcd (%) for $C_9H_{14}O_{10}N_4Cu_2$: C, 23.23; H, 3.03; N, 12.04. Found (%): C, 23.21; H, 3.05; N, 12.07. Main IR bands (KBr, $cm^{-1}$): 3457s, 1635m 1607w, 1569m, 1477m, 1450m, 1418m, 1310s, 1251w, 1207w, 1013s, 932w.

**$[Co_2(OH)(TZI)(H_2O)_2]_n·4nH_2O$** (**2**). A procedure similar to that for **1** was followed to prepare **2** using $Co(NO_3)_2·6H_2O$ instead of $Cu(NO_3)_2·3H_2O$. Red crystals were obtained. Yield, 68% based on Co. Elem anal. Calcd (%) for $C_9H_{16}O_{11}N_4Co_2$: C, 22.80; H, 3.40; N, 11.82. Found (%): C, 22.82; H, 3.43; N, 11.79. Main IR bands (KBr, $cm^{-1}$): 3415s, 1623m, 1579w, 1494m, 1429m, 1413m, 1380s, 1229w, 1160w, 1111s, 903w.

**$[Ni_2(OH)(TZI)(H_2O)_2]_n·4nH_2O$** (**3**). A procedure similar to that for **1** was followed to prepare **3** using $Ni(NO_3)_2·6H_2O$ instead of $Cu(NO_3)_2·3H_2O$. Green microcrystals were obtained. Our attempts to get single crystals of **3** by different methods did not succeed. Yield, 64% based on Ni. Elem anal. Calcd (%) for $C_9H_{16}O_{11}N_4Ni_2$: C, 22.82; H, 3.41; N, 11.83. Found (%): C, 22.84; H, 3.44; N, 11.86. Main IR bands (KBr, $cm^{-1}$): 3416s, 1624m, 1578w, 1489m, 1430m, 1411m, 1376s, 1224w, 1158w, 1110s, 905w.

### Crystal structure analysis

Diffraction data for **1** and **2** were collected at 293 K on a Bruker Apex II CCD area detector equipped with graphite-monochromated Mo Kα radiation ($\lambda$ = 0.71073 Å). Empirical absorption corrections were applied using the SADABS program.[12] The structures were solved by the direct method and refined by the full-matrix least-squares method on $F^2$, with all non-hydrogen atoms refined with anisotropic thermal parameters.[13] All the hydrogen atoms attached to carbon atoms were placed in calculated positions and refined using the riding model. The coordinated water hydrogen atoms were located from the difference maps. The uncoordinated water hydrogen atoms could not be modeled owing to the disorder and the limited quality of dataset. A summary of the crystallographic data, data collection, and refinement parameters are provided in Table 1.

**Table 1** Crystal data and structure refinement for compounds **1** and **2**

| Compounds | 1 | 2 |
|---|---|---|
| Empirical formula | $Cu_2C_9H_{14}N_4O_{10}$ | $Co_2C_9H_{16}N_4O_{11}$ |
| Formula weight | 465.32 | 474.12 |
| Crystal system | Monoclinic | Monoclinic |
| Space group | $P2_1/m$ | $P2_1/m$ |
| $a$ /Å | 10.0150(9) | 10.1792(15) |
| $b$ /Å | 6.6124(5) | 6.7279(9) |
| $c$ /Å | 12.4721(11) | 12.8158(18) |
| α /° | 90 | 90 |
| $\beta$ /° | 109.412(2) | 111.698(4) |
| γ /° | 90 | 90 |
| $V$ /Å$^3$ | 778.99(11) | 815.5(2) |
| $Z$ | 2 | 2 |
| $Dc$ (g $m^{-3}$) | 1.984 | 1.931 |
| $\mu$ ($mm^{-1}$) | 3.977 | 2.102 |
| $F$(000) | 468 | 480 |
| Reflections collected | 2553 | 14710 |
| Unique reflections | 1449 | 2013 |
| GOF on $F^2$ | 1.002 | 1.025 |
| $R_{int}$ | 0.0877 | 0.0236 |
| $R_1$ [I>2σ(I)] | 0.1050 | 0.0345 |
| $wR_2$ (all data) | 0.2989 | 0.0983 |

## Results and discussion

Synthesis. Compounds **1**-**3** were synthesized by the reactions of metal(II) nitrate and $H_3TZI$ ligand in mixed aqueous acetonitrile at 150°C. However, a Cu(II) MOF with TZI (reference 11a) was obtained by the reactions of copper(II) nitrate and $H_3TZI$ ligand in an N,N-dimethylformamide/ethanol solution at 80°C. The compositions and structures in **1**-**3** are quite different from those for a Cu(II) compound with reference 11a. Notably, we report the first examples of novel coordination modes of this ligand. The coordination modes of the TZI ligand for the previous compounds have been given elsewhere.[11]

The IR spectra of **1**-**3** show a broad absorption band at 3415-3457 $cm^{-1}$, which should be ascribed to the $v$(O-H) vibration of free and coordinated water molecules and the hydroxy groups. All compounds exhibit characteristic asymmetric ($v_{as}$) and symmetric ($v_s$) absorptions of the carboxylate groups [14] and the tetrazole groups absorption peaks at 1400-1500 $cm^{-1}$.[15]

PXRD of **1**-**3:** PXRD experiments have been carried out for **1**-**3** to confirm the phase purity of the bulk samples. In **1** and **2**, the experimental and simulated PXRD patterns (Fig. S1, Fig. S2) were in good agreement with each other, indicating the phase purity of the as-synthesized products. We failed in obtaining single crystals of **3** for X-ray crystallographic analysis. However, the PXRD pattern of **3** is in good agreement with that calculated from the single-crystal data of **2,** suggesting **2** and **3** are isomorphous (Fig. S2).

**Description of the Structures.** Compounds **1** and **2**. X-ray crystallographic analyses revealed that compounds **1** and **2** are isostructural and exhibit three-dimensional frameworks in which 1D magnetic Δ-chains are connected by TZI spacers. The coordination environment of the metal ions are shown in Fig. 1a. There are two crystallographically independent metal(II) ions in the asymmetric unit. Cu1/Co1 assumes a distorted octahedral [N$_2$O$_4$] coordination geometry defined by two tetrazolate nitrogen atoms (N1B and N1C), three carboxylate oxygen atoms (O1, O2 and O4A), and one $\mu_3$-OH group oxygen atoms (O5). The M1-N/O distances range from 1.872(13) to 2.242(12) Å for Cu1 and 1.996(3) to 2.262(2) Å for Co1. Cu1 may also be as an axially compressed octahedron, in which the equatorial plane contains O1, N1B, O5, N1C with bond distance of 2.206-2.42 Å and the apical positions are O2 and O4 with bond distance of 2.001 and 1.872 Å, respectively. This feature is pertinent to the magnetic properties. The Cu2/Co2 are located at a inversion center in similar an axially elongated octahedral [N$_2$O$_4$] environments. The equatorial plane is defined by two $\mu_3$-OH groups oxygen atoms (O5, O5I) and two tetrazolate nitrogen atoms (N2C, N2E), and the axial sites were occupied by two coordinated water molecules (O6, O6D). It was noted that the coordinated water molecules (O6) is at 2.508(2) Å from Cu2, suggesting weak coordination. If this is not included, the geometry of Cu2 may be described as a distorted quadrilateral. The equatorial M–N/O distances (av. 1.965(8) Å for **1** and 2.079(1) Å for **2**) are somewhat shorter than the axial M–O distances (2.508(2) Å for **1** and 2.140(2) Å for **2**. Adjacent the equatorial planes intrachain are slanted towards each other with the average angle of 22.07° for **1** and 25.75° for **2** between the equatorial planes.

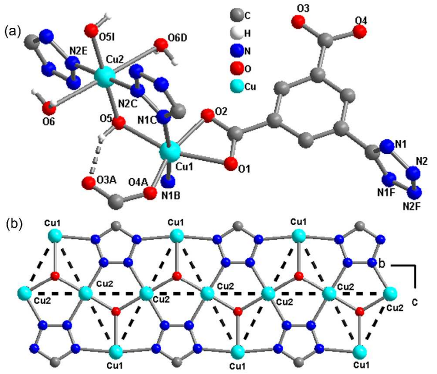

**Fig. 1** (a) Local coordination environments in compound 1. (b) Infinite strip-shaped Δ-chain topology based on corner-sharing M$_3$($\mu_3$-OH) triangle used to assemble 1. Symmetry codes: A x-1,y,z; B -x+1,y-1/2,-z+2; C -x+1,-y+2,-z+2; D -x,-y+2,-z+1; E x-1,y,z-1; F x,-y+3/2,z; I -x,y-1/2,-z+1.

The central hydroxyl group uses its oxygen atom binding three M ions, generating an isosceles triangle [M$_3$($\mu_3$-OH)] with the M1···M2 distances of 3.562(2) and 3.5869(6) Å, and M2···M2 of 3.3062(3) and 3.3640(4) Å for **1** and **2**, respectively, and M-O-M angle of about 117.0-117.4° for **1** for and 108.9-119.4° for **2**. The $\mu_3$-OH oxygen atom is out of the mean basal plane by 0.3472(3) Å for **1** and 0.4223(3) Å for **2**, which results in a non-coplanar [M$_3$($\mu_3$-OH)] triangle. The [M$_3$($\mu_3$-OH)] triangles are linked by sharing the M2 ions and adjacent M1 ions are bridged by μ-N1,N1F- tetrazolate groups to form an infinite strip-shaped Δ-chain along the *b* direction (Fig. 1b). It should be noted that a few examples of such Δ-chain topology have been reported so far.[9,10] The Δ-chains in **1** and **2** were interlinked by TZI ligands to generate the 3D network framework with the shortest interchain M···M separations spanned by the TZI ligands being 7.907(4) Å and 8.141(1) Å, respectively (Fig. 2a). Each TZI ligand serves as a $\mu_6$- bridging mode, with the chelated carboxylate group binding one M1 ions and the other carboxylate group binding one symmetry related M1 atom in a monocarboxylate mode, meanwhile, the tetrazolate group bridging four meatal ions (one pair of M1 and one pair of M2). The uncoordinated oxygen atom (O3A) of the monodentate catboxylate group hydrogen-bonded to a $\mu_3$-OH group oxygen atom (O5) with O5-H5B···O3A = 148.6(8)°, H5B···O3A = 1.974(2) Å and O5···O3A = 2.736(2) Å for **1**; O5-H5B···O3A = 167.9(2)°, H5B···O3A = 2.136(6) Å and O5···O3A = 2.792(6) Å for **2**.

From the view of topology, the $\mu_3$-OH group and TZI ligand serve as 3- and 6-connected nodes, respectively, to join three M(II) ions (one M1 and two M2) and six M(II) ions (four M1 and two M2). The M1 and M2 play the 5- and 4-connected role, respectively, to link the TZI nodes and $\mu_3$-OH nodes (2 tetrazolate + 2 carboxylate + 1 $\mu_3$-OH nodes for M1 and 2 tetrazolate + 2 $\mu_3$-OH nodes for M2). Thus, the overall 3D network could be described as a 4-nodal (3,4,5,6)-connected net with the point symbol of $(4^3)(4^46^2)(4^76^8)$ (Fig. 2b).

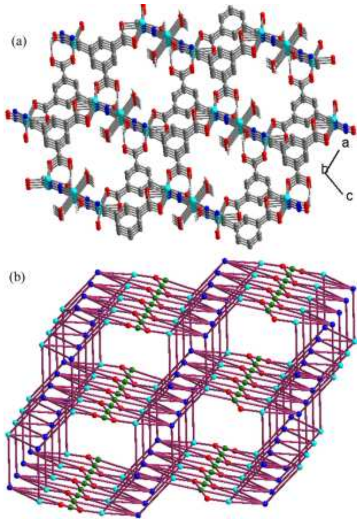

**Fig. 2** (a) A view of the 3D structure of 1. (b) View of 3D (3,4,5,6)-connected net with $(4^3)(4^46^2)(4^66^4)(4^76^8)$ topology for 1 (Cu1 turquiose, Cu2 green, O red, TZI blue).

## Magnetic Properties.

Compounds **1**–**3**. The magnetic susceptibility (χ) of compound **1** was measured on a pure polycrystalline sample under 1000 Oe in the range 2-300 K (Fig. 3a). The $\chi T$ value of per Cu$_2$ at room temperature is about 0.74 emu K mol$^{-1}$, being close to the value expected for two magnetically isolated Cu(II) ion. As the temperature is lowered, the $\chi T$ values first decrease to a minimum at 28 K and then show rapid increases to a maximum of 0.79 cm$^3$ mol$^{-1}$ K at 3.5 K, and finally decreases again down to 2 K, while the $\chi$ value first increases and then decreases. The data above 130 K follow the Curie-Weiss law with $C$ = 0.78 emu K mol$^{-1}$ and $\theta$ = -14.1 K. This behavior of the $\chi T$-T plot is characteristic of spin-canted antiferromagnetism, while a peak at 2.5 K in the $\chi$-T curve is characteristic for the antiferromagnetic ordering. However, so far, no appropriate theoretical model was used to estimate the magnetic exchange parameters in the complicated system containing the magnetic strip-shaped Δ-chain with mixed double ($\mu_3$-OH and $\mu_4$-tetrazolate) bridges.

In order to confirm the actual coupling nature for compound **1**, the zero-field-cooled (ZFC) and field-cooled (FC) magnetization were measured under 20 Oe in the range of 2-20 K. (Fig. 3b). The FC and ZFC are identical and show a peak at 2.5 K, implying the short-range order of spins in antiferromagnetic coupling. Furthermore, the ac susceptibility shows a frequency-independent maximum at 6 K in the real ($\chi'$) component (Fig. 3c), and no signal was observed in imaginary component($\chi''$), supporting the onset of antiferromagnetic ordering below $T_c$ = 2.6 K.

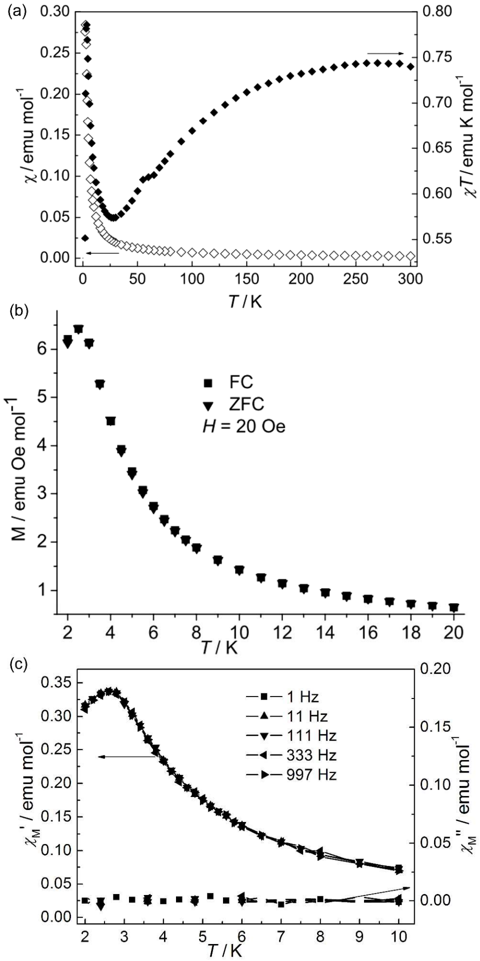

**Fig. 3** (a) Magnetic susceptibility of **1** plotted as $\chi T$ vs $T$ and $\chi$ vs $T$ curves at 1 kOe. (b) The FCM and ZFCM curves at 20 Oe for **1**. (c) Magnetic susceptibility (AC) obtained at 3 Oe field for **1**. The lines are guides.

The isothermal magnetization curve at 2 K first increases rapidly and then increases showly to 0.61 Nβ at 50 kOe with increased field, which is much lower than the saturation value of two Cu(II) ions (2.00 Nβ) (Fig. 4a), confirming a canted antiferromagnet. The linear region in high field was extrapolated to zero field, which gives a magnetization value of 0.415 $N\beta$. That value could be taken as the weak magnetization ($M$r) contribution arising from spin canting. Thus, the canting angle (γ) can be roughly estimated by sin(γ) = $M_r/M_S$ to be 11.98°($M_S$ = 2.0 $N\beta$ for two Cu(II) ions).[1a] In the low-field region, the magnetization curve presents a sigmoid shape, which indicates a metamagnetic behavior. The critical field is estimated to be about 1.7 kOe according to the d$M$/d$H$ derivative plot (Fig. 4a). Metamagnetism is also confirmed by the field-cooled (FC) magnetizations under different fields (Fig. 4b). The FC plot displays a maximum under 1.5 kOe at about 2.3 K, supporting the occurrence of antiferromagnetic ordering. As the field is lifted, the maximum shifts toward lower temperatures and becomes less prominent. When the external field is increased to 2.5 kOe, the maximum disappears, indicating that the antiferromagnetic interactions were overcome by a high field.[16] The magnetization loop was measured by cycling of the field between -50 - 50 kOe at 2 K. No hysteresis was observed upon cycling of the field between -50 - 50 kOe at 2 K (Fig. S3).

According to the structural data, Cu1 assumes an axially compressed octahedron, while Cu2 is an axially elongated octahedron. So, the unpaired electron is in dz$^2$ orbital of Cu1 but in dx$^2$-y$^2$ of Cu2. So that it is ferromagnetic coupling between Cu1 and Cu2 ions. It is well known that the interaction in the Cu(II) systems is sensitive to the Cu-O-Cu angle, with large bridging angles (>97.5°) transmitting antiferromagnetic coupling.[17] Thus, O5 and tetrazole ligand mediate the antiferromagnetic coupling between Cu2 ions, because **1** has a larger Cu2-O-Cu2 angle [117.37°] in equatorial plane and tetrazole provides a two - atoms bridge mediating antiferromagnetic interaction in spin polarization mechanism. The interaction intrachain between Cu1 ions is very weak by tetrazole groups, which can be neglected. The antiferromagnetic coupling is much stronger than the ferromagnetic coupling, so the spin at Cu1 is frustrated. Just for this reason, this system shows the spin-canting phenomenon. The canting source is from Cu1 and the canting angle should be larger than the usual antiferromagnetic system.

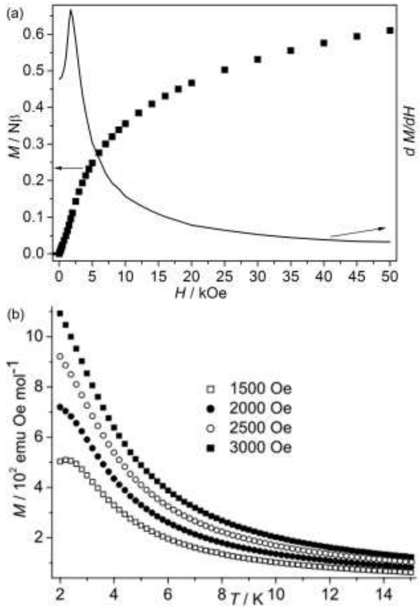

**Fig. 4** (a) Isothermal magnetization curves at 2 K for **1**; (b) FC magnetization curves for **1** at different fields.

The magnetic susceptibility ($\chi$) of **2** is shown in Fig. 5a. The $\chi$T value per Co2 at room temperature is about 6.42 emu K mol$^{-1}$, which is much larger than the spin-only value of 3.75 emu K mol$^{-1}$ for three non-interacting octahedral Co(II) ions (S = 3/2, g = 2.00), owing to the strong orbital contribution. As the temperature is lowered, the $\chi T$ values decreases continuously, while the $\chi$ value increases slowly to an approximate plateau at about 9 K and then increases rapidly upon further cooling to 2 K. This shape of the plots may be attributed to spin canting, due to the alignment of these antiferromagnetic interactions in an isosceles triangle. The data above 200 K follow the Curie-Weiss law with $C$ = 6.72 emu K mol$^{-1}$ and $\theta$ = -14.3 K. The decrease of $\chi T$ with decreased temperature indicates antiferromagnetic coupling between Co(II) ions. But the negative $\theta$ value is not necessary for the antiferromagnetic interactions because a single octahedral Co(II) ion has the effects of the spin-orbital coupling. The isothermal magnetization curve measured at 2 K (Fig. 5b) also supports the spin-canting of **2**. The magnetization first increases rapidly and then increases slowly with the 0.75 Nβ at 50 kOe with increased field, which is much lower than the saturation value of two Co(II) ions. These features are consistent with the antiferromagnetic interactions in the intrachain. The nonlinearity of the low-field range can be due to spin canting. Thermal ac susceptibilities were measured on **2** under a zero dc field at different frequencies (Fig. S4). The real ($\chi'$) component exhibits a frequency-independent without the maximum and no signal was observed the imaginary component($\chi''$), suggesting magnetic ordering not occurring above 2K. The intrachain magnetic behaviors are similar to those of previous compounds with similar Δ-chains based on mixed double bridges ($\mu_3$-OH and $\mu_4$-tetrazolate),[9] which also are ascribed to the spin canting antiferromagnetic coupling.

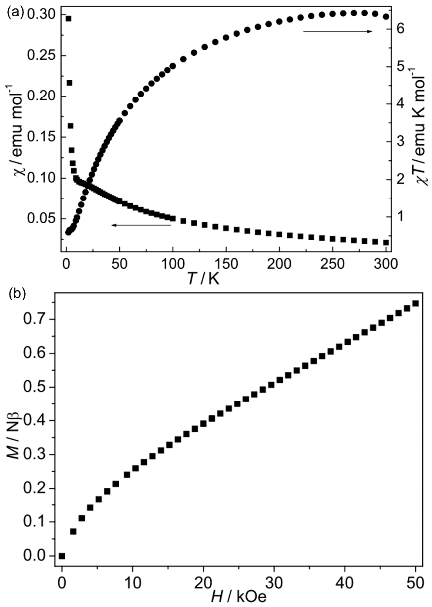

**Fig. 5** (a) The $\chi T$ and $\chi$ vs $T$ plot of **2** at 1 kOe; (b) Field-dependent isothermal magnetization curve of **2** at 2 K.

The overall magnetic behavior of **3** is similar to that of **2**. The $\chi T$ value per $Ni_2$ at 300 K is 2.54 emu K mol$^{-1}$, corresponding to a S = 1 spin with g >2 (Fig. 6a). Upon cooling, the $\chi T$ values decreases continuously, while the $\chi$ value increases slowly to an approximate plateau and then increases rapidly upon further cooling to 2 K. This behavior is characteristic of a canted spin system. The data above 120 K follow the Curie-Weiss law with $C$ = 2.92 emu K mol$^{-1}$ and $\theta$ = -44.3 K. The negative value of $\theta$ indicates antiferromagnetic coupling in the high temperature range. The magnetization curve increases nonlinearly with the 0.32 Nβ at 50 kOe with increased field (Fig. 6b), which is far from the saturation value, in agreement with that expected for a spin-canted antiferromagnet. Frequency independent behavior was observed in thermal ac susceptibility curves (Fig. S5). No maximum in the real component ($\chi'$) and no imaginary signal ($\chi''$) were observed, indicating the antiferromagnetic interaction between Ni(II) ions and the absence of long-range ordering above 2 K.

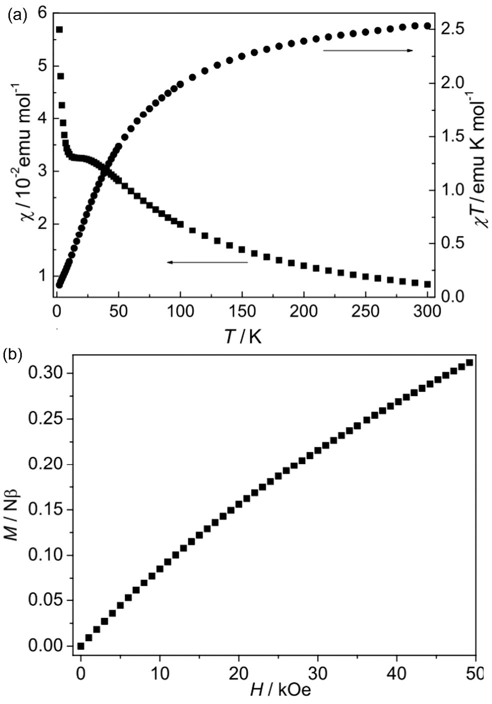

**Fig. 6** (a) The $\chi T$ and $\chi$ vs $T$ plot of **3** at 1 kOe; (b) Field-dependent isothermal magnetization curve of **3** at 2 K.

Spin canting can be constructed by using Δ-chain containing triangle motifs with antisymmetric magnetic exchange and/or single-ion magnetic anisotropy. The isostructural compounds **1**-**3** with magnetic Δ-chain all exhibit intrachain spin canted anferromagnetic interactions but show distinct bulk properties: compound **1** shows spin canting, antiferromagnetic ordering and field-induced metamagnetism, whereas compounds **2** and **3** exhibit canted antiferromagnetic coupling without magnetic ordering above 2 K. The canted antiferromagnetic coupling in **1** arised from the competition of antiferromagnetic and ferromagnetic interactions between spins, which results in uncompensated residual spins. The spin-competing antiferromagnetic interaction is presented in this system due to the magnetic Δ-chains. As for **2** and **3**, the Co(II) and Ni(II) ions have spin-orbital coupling and single-ion anisotropy. The spin-orbital coupling destroys the competing interaction in the system, and results in spin canting, and single-ion anisotropy (one of the origins of spin-canting) of Co(II) ion favours spin canting. The occurrence of 3D magnetic ordering may be related to the intrachain and/ or interchain interactins. Generally, the intrachain factors can determine the occurrence of ordering and the ordering temperature.[18] The ordering temperature can also be evoked by interchain exchange and the degree of spin canting. Two interchain interactions are essential for magnetic ordering: one is the superexchange interactions interchains through weak bonds, which disappears very rapidly as the distance increases, and the other is dipolar interactions interchains through space, which has long-range effects. The magnetic difference among compounds **1**-**3** is related to interchain and/ or intrachain interaction. It is difficult to make detailed comparisons between the two series owing to the wide different nature of bridges and spin centers.

## Conclusions

Three new spin canting magnets with corner-sharing $M_3(\mu_3\text{-OH})$ isosceles triangle Δ-chain were synthesized and structurally and magnetically characterized. The isostructural compounds **1-3** show 3D structures assembled by the TZI ($H_3TZI$ = 5-(1H-tetrazol-5-yl)isophthalic acid) ligands linking Δ-chains, which represent the rare (3,4,5,6)-connected 4-nodal net topology with the point symbol $(4^3)(4^46^2)(4^66^4)(4^76^8)$. Magnetic investigations on three compounds reveal that all exhibit intrachain canted antiferromagnetic interactions. **1** shows the coexistence of spin canting, metamagnetism and antiferromagnetic ordering, whereas **2** and **3** exhibit canted antiferromagnetic coupling without magnetic ordering above 2 K. More interesting, the coexistence of several magneic behaviors was observed in **1**, and the origin of spin canting was discussed. Especially, compounds **1** and **3** are the first Cu(II) and Ni(II) compounds with such magneic behaviors above 2 K in the series. This work provide a good example for magnetic studies with similar structures and different spin carriers to research magneto-structural correlations.

## Acknowledgements

We are thankful for the financial support from NSFC (21201069) and the Natural Science Foundation of Anhui Province (1308085QB23).

## Notes and references

*College of Chemistry and Materials Science, Huaibei Normal University, Anhui 235000, China, E-mail：zhangxiumeilb@126.com

Electronic Supplementary Information (ESI) available: [The data can be obtained free of charge via <http://www.ccdc.cam.ac.uk/conts/retrieving.html>, or from the Cambridge Crystallographic Data Centre, 12 Union Road, Cambridge CB2 1EZ, UK; fax:(+44) 1223-336-033; or e-mail: deposit@ccdc.cam.ac.uk and Fig. S1–S5]. See DOI: 10.1039/b000000x/. CCDC reference Number: 1409334 (**1**), 1409333 (**2**). For ESI and crystallographic data in CIF or other electronic format See DOI: 10.1039/x0xx00000x

1 (a) O. Kahn. Molecular Magnetism, VCH: Weinheim, Germany, 1993; (b) J.S. Miller. *Adv. Mater*. 2002, **14**, 1105; (c) J.S. Miller and M. Drillon. Magnetism: Molecules to Materials; Wiley-VCH: Weinheim, Germany, 2002−2005; *Vols*. **I−V**; (d) R.L. Carlin. Magnetochemistry, Springer, Berlin-Heidelberg, 1986; (e) C. Coulon, H. Miyasaka and R. Clérac. *Struct. Bonding*, 2006, **122**, 163.
2 (a) D.F. Weng, Z.M. Wang and S. Gao. *Chem. Soc. Rev*. 2011, **40**, 3157; (b) J.R. Li, R.J. Kuppler and H.-C. Zhou. *Chem. Soc. Rev*. 2009, **38**, 1477; (c) P. Zhang, Y.N. Guo and J. Tang, *Coord. Chem. Rev*. 2013, **257**, 1728; (d) X.Y. Wang, C. Avendano and K.R. Dunbar, *Chem. Soc. Rev*. 2011, **40**, 3213.
3 (a) Y. Hu, M. Zeng, K. Zhang, S. Hu, F. Zhou and M. Kurmoo. *J. Am. Chem. Soc*. 2013, **135**, 7901; (b) S. Xiang, X. Wu, J. Zhang, R. Fu, S. Hu and Zhang, X. *J. Am. Chem. Soc*. 2005, **127**, 16352; (c) P.L. Arnold. *Nat. Chem.* 2012, **4**, 967; (d) D. Gatteschi, R. Sessoli. *Angew.*

*Chem., Int. Ed.* 2003, **42**, 268.

4 (a) T. Moriya. *Phys. Rev.* 1960, **117**, 635; (b) I. Dzyaloshinsky. *J. Phys. Chem. Solids*. 1958, **4**, 241; (c) T. Moriya. *Phys. Rev.*, 1960, **120**, 91.

5 (a) M.B. Hastings. *Phys. Rev. B* 2001, **63**, 014413/1; (b) D. Shao, S.-L. Zhang. X.-H. Zhao and X.-Y. Wang. *Chem. Commun.*, 2015, **51**, 4360; (c) B. Li, Z. Li, R.-J. Wei, F. Yu, X. Chen, Y.-P. Xie, T.-L. Zhang and J. Tao. *Inorg. Chem.* 2015, **54**, 3331; (d) B.M. Bartlett and D.G.Nocera, *J. Am. Chem. Soc.* 2005, **127**, 8985; (e) D. Papoutsakis, D. Grohol and D.G. Nocera, *J. Am. Chem. Soc.* 2002, **124**, 2647.

6 (a) B. Deviren and M. Keskin. *Phys. Lett. A*, 2010, **374**, 3119; (b) N. Motokawa, S. Matsunaga, S. Takaishi, H. Miyasaka, M. Yamashita and K.R. Dunbar, *J. Am. Chem. Soc.*, 2010, **132**, 11943; (c) W.-W. Sun, C.-Y. Tian, X.-H. Jing, Y.-Q. Wang and E.-Q. Gao, *Chem. Commun.*, 2009, 4741; (d) X.-M. Zhang, Y.-Q. Wang, Y. Song and E. -Q. Gao. *Inorg. Chem.* 2011, **50**, 7284.

7 (a) W. Ouellette, A.V. Prosvirin, K. Whitenack, K.R. Dunbar and J. Zubieta. *Angew. Chem.* 2009, **121**, 2174; *Angew. Chem. Int. Ed.* 2009, **48**, 2140.. (b) M. Dinca, A.F. Yu and J.R. Long. *J. Am. Chem. Soc.* 2006, **128**, 8904; (c) G. Aromí, L. A, Barrios, O. Roubeau, P. Gamez, *Coord. Chem. Rev.* 2011, **255**, 485; (d) X.-B. Li, J.-Y. Zhang, Y.-Q. Wang, Y. Song and E.-Q. Gao. *Chem. Eur. J.* 2011, **17**, 13883; (e) X.-B. Li, G.-M. Zhuang, X. Wang, K. Wang and Gao. E.-Q. *Chem. Commun.,* 2013, **49**, 1814; (f) Q.-X. Jia, Y.-Q. Wang, Q. Yue, Q.-L. Wang and E.-Q. Gao. *Chem. Commun.*, 2008, 4894. (g) X.-M. Zhang, P. Li, W. Gao, J.-P. Liu and E.-Q. Gao. *Dalton Trans.*, 2015, **44**, 511.

8 (a) H. Tian, Q.-X. Jia, E.-Q. Gao and Q.-L. Wang. *Chem. Commun*., 2010, **46**, 5349; (b) M. Kurmoo. *Chem. Soc. Rev.* 2009, **38**, 1353; (c) Q. Sun, A.-L. Cheng, Y.-Q. Wang, Y. Ma and E.-Q. Gao. *Inorg. Chem.*, 2011, **50**, 8144; (d) Y.-Z. Zheng, M.-L. Tong, W. X. Zhang and X.-M. Chen, *Angew. Chem., Int. Ed.* 2006, **45**, 6310; (e) S. R. Caskey, A.G. Wong-Foy and A. J.Matzger. *J. Am. Chem. Soc.* 2008, **130**, 10870; (f) E.A. Nytko, J. S. Helton, P. Müller and D.G. Nocera, *J. Am. Chem. Soc.* 2008, **130**, 2922.

9 (a) R.-X. Yao, Y.-L. Qin, F. Ji, Y.-F. Zhao and X.-M. Zhang. *Dalton Trans*., 2013, 42, 6611; (b) W.-C. Song, Tao, J.; T.-L. Hu, Y.-F. Zeng, X.-H. Bu. *Dalton Trans*., 2011, **40**, 11955. (c) E.-C. Yang, Z.-Y. Liu, X.-Y. Wu and X.-J. Zhao. *Chem. Commun*., 2011, **47**, 8629; (d) D.-S. Liu, Y. Sui, T.-W. Wang, C.-C. Huang, J.-Z. Chen, X.-Z. You, *Dalton Trans.*, 2012, **41**, 5301.

10 E.-C. Yang, Z.-Y. Liu, X.-Y. Wu, H. Chang, E.-C. Wang, X.-J. Zhao. *Dalton Trans.*, 2011, **40**, 10082.

11 (a) F. Nouar, J. F. Eubank, T. Bousquet, L. Wojtas, M. J. Zaworotko and M. Eddaoudi. *J. Am. Chem. Soc.,* 2008, **130**, 1833. (b) A. J. Calahorro, A. Salinas-Castillo, J. M. Seco, J. Zuñiga, E. Colacioa and A. Rodríguez-Diéguez, *CrystEngComm*, 2013, **15**, 7636. (c) Z.-R. Qu, Z. Xing, B. -Z. Wu, X. -Z. Li, and G. -F. Han. *Z. Anorg. Allg. Chem.* 2009, **635**, 39. (d) J. Jia, J.-N. Xu, S.-Y. Wang, P.-C. Wang, L.-J. Gao, M. Yu, Y. Fan and L. Wang. *CrystEngComm*, 2015,**17**, 6030.

12 Sheldrick, G. M. Program for Empirical Absorption Correction of Area Detector Data; University of Göttingen, Germany, 1996.

13 Sheldrick, G. M. SHELXTL Version 5.1. Bruker Analytical X-ray Instruments Inc., Madison, Wisconsin, USA, 1998.

14 (a) K. Nakamoto, Infrared and Raman Spectra of Inorganic and coordination Compounds, 5th ed. Part B; John Wiley, New York, 1997. (b) G. B. Deacon and R. J. Phillips, *Coord. Chem. Rev*., 1980, **33**, 227.

15 (a) Y. C. Qiu, H. Deng, J. X. Mou, S. H. Yang, M. Zeller, S. R. Batten, H. H. Wu and J. Li, *Chem. Commun*., 2009, 5415. (b) Y. C. Qiu, Y. H. Li, G. Peng, J. B. Cai, L. M. Jin, L. Ma, H. Deng, M. Zeller and S. R. Batten, *Cryst. Growth Des.*, 2010, **10**, 1332. (c) B. Liu, Y. C. Qiu, G. Peng and H. Deng, *CrystEngComm*., 2010, **12**, 270.

16 Carlin, R. L. *Magnetochemistry*, Springer, Berlin, 1986.

17 (a) R. W. Jotham, S. F. A. Kettle, *Inorg. Chim. Acta* 1970, **4**, 145. (c) V. H. Crawford, H. W. Richardson, J. R. Wasson, D. J. Hodgson, W. E. Hatfield, *Inorg. Chem*. 1976, **15**, 2107. (b) Y.-f. Song, C. Massera, O. Roubeau, P. Gamez, A. M. M. Lanfredi, J. Reedijk, *Inorg. Chem*. 2004, **43**, 6842.

18 (a) J. S. Miller. *Chem. Soc. Rev.*, 2011, **40**, 3266; (b) M. Drillon, P. J. Panissod. *Magn. Mater*. 1998, **188**, 93. (c) P. Panissod and M. Drillon. In Magnetism-From Molecules to Materials; J. S. Miller, M. Drillon, Eds.; Wiley-VCH: Weinheim, 2002;Vol. **IV**, pp 233 269.